AIP | The Journal of Chemical Physics

The electron-furfural scattering dynamics for 63 energetically open electronic states

Romarly F. da Costa, Márcio T. do N. Varella, Márcio H. F. Bettega, Rafael F. C. Neves, Maria Cristina A. Lopes, Francisco Blanco, Gustavo García, Darryl B. Jones, Michael J. Brunger, and Marco A. P. Lima

Citation: The Journal of Chemical Physics **144**, 124310 (2016); doi: 10.1063/1.4944616
View online: http://dx.doi.org/10.1063/1.4944616
View Table of Contents: http://scitation.aip.org/content/aip/journal/jcp/144/12?ver=pdfcov
Published by the AIP Publishing

The electron-furfural scattering dynamics for 63 energetically open electronic states

Romarly F. da Costa,[1,2] Márcio T. do N. Varella,[3] Márcio H. F. Bettega,[4] Rafael F. C. Neves,[5,6] Maria Cristina A. Lopes,[6] Francisco Blanco,[7] Gustavo García,[8] Darryl B. Jones,[9] Michael J. Brunger,[9,10] and Marco A. P. Lima[1,a)]

[1]*Instituto de Física "Gleb Wataghin," Universidade Estadual de Campinas, Campinas, São Paulo 13083-859, Brazil*
[2]*Centro de Ciências Naturais e Humanas, Universidade Federal do ABC, Santo André, São Paulo 09210-580, Brazil*
[3]*Instituto de Física, Universidade de São Paulo, CP 66318, São Paulo, São Paulo 05315-970, Brazil*
[4]*Departamento de Física, Universidade Federal do Paraná, CP 19044, Curitiba, Paraná 81531-990, Brazil*
[5]*Instituto Federal do Sul de Minas Gerais, Campus Poços de Caldas, Minas Gerais, Brazil*
[6]*Departamento de Física, Universidade Federal de Juiz de Fora, Juiz de Fora, MG 36036-900, Brazil*
[7]*Departamento de Física Atómica, Molecular y Nuclear, Universidad Complutense de Madrid, Madrid E-28040, Spain*
[8]*Instituto de Física Fundamental, CSIC, Serrano 113-bis, 28006 Madrid, Spain*
[9]*School of Chemical and Physical Sciences, Flinders University, GPO Box 2100, Adelaide, South Australia 5001, Australia*
[10]*Institute of Mathematical Sciences, University of Malaya, 50603 Kuala Lumpur, Malaysia*

(Received 14 January 2016; accepted 8 March 2016; published online 29 March 2016)

We report on integral-, momentum transfer- and differential cross sections for elastic and electronically inelastic electron collisions with furfural ($C_5H_4O_2$). The calculations were performed with two different theoretical methodologies, the Schwinger multichannel method with pseudopotentials (SMCPP) and the independent atom method with screening corrected additivity rule (IAM-SCAR) that now incorporates a further interference (I) term. The SMCPP with N energetically open electronic states (N_{open}) at either the static-exchange (N_{open} ch-SE) or the static-exchange-plus-polarisation (N_{open} ch-SEP) approximation was employed to calculate the scattering amplitudes at impact energies lying between 5 eV and 50 eV, using a channel coupling scheme that ranges from the 1ch-SEP up to the 63ch-SE level of approximation depending on the energy considered. For elastic scattering, we found very good overall agreement at higher energies among our SMCPP cross sections, our IAM-SCAR+I cross sections and the experimental data for furan (a molecule that differs from furfural only by the substitution of a hydrogen atom in furan with an aldehyde functional group). This is a good indication that our elastic cross sections are converged with respect to the multichannel coupling effect for most of the investigated intermediate energies. However, although the present application represents the most sophisticated calculation performed with the SMCPP method thus far, the inelastic cross sections, even for the low lying energy states, are still not completely converged for intermediate and higher energies. We discuss possible reasons leading to this discrepancy and point out what further steps need to be undertaken in order to improve the agreement between the calculated and measured cross sections. © *2016 AIP Publishing LLC.* [http://dx.doi.org/10.1063/1.4944616]

I. INTRODUCTION

Over the past three decades the interest in developing new and/or improved (especially towards cost-effectiveness and sustainability) technologies, notably for lignocellulosic biomass conversion to biofuels and other biomaterials,[1] has been boosted by a scenario in which the growing worldwide demand for energy[2] must be met while addressing concerns about global climate changes. Among the challenges to be overcome, the natural resilience of plant cell walls, in particular to the destructive action of microbial and enzymatic processes (a property collectively know as "biomass recalcitrance"), is nowadays recognized as being largely responsible for the high cost of lignocellulose conversion into biomaterials that possess a high added value. Aiming to address this question, theoretical and experimental investigations revealed that free-electrons and radical species formed within atmospheric-pressure plasmas have the ability to contribute to the deconstruction of biomass.[3–6] In this context, low-energy electrons produced within the plasma environment have the potential to induce breakage of chemical bonds through dissociative electron attachment, electron-impact excitation, and other fragmentation processes.

Motivated by this body of evidence, we have recently carried out several joint experimental and theoretical studies on electron collisions with phenol, a subunit of lignin (an important biomass component), reporting total, elastic, momentum transfer, vibrational and electronic inelastic cross

a)Electronic mail: maplima@ifi.unicamp.br

sections.[7–10] We have presented experimental results including vibrational, electronic excitation, and total cross sections for intermediate energies from 15 up to 50 eV. On the theoretical side, we have calculated elastic, momentum transfer, electronically inelastic and total cross sections, with particular attention on the convergence of the multichannel coupling, in order to assess how the increase in the number of excited states included in the open-channel space impacts the behaviour of the cross sections.

Following the path of plasma applications to biomass disassembly, we considered furfural as another good candidate for an electron scattering investigation. Indeed, furfural is a molecule commonly used in industries and can be obtained from biomass, specifically from one of its components, the hemicellulose fraction of lignocellulose (see discussion by Ferreira da Silva *et al.*[11]). The first two papers in respect to this subject were on the electronic excitation spectrum[11] and on the vibrational excitation[12] by electron impact of furfural. In this paper we will present results for the elastic integral cross sections (ICSs), elastic momentum transfer cross sections (MTCS), elastic and inelastic differential cross sections (DCSs), and total cross sections (TCSs) for electron scattering by the furfural molecule, focusing on the analysis of the influence of multichannel coupling effects.

The paper is organized in such a way that in Section II we present a summary of the theoretical methods used in the paper, followed by Section III that contains specific details of their applications. There are two stable conformations of furfural, *cis* and *trans*, the latter being more stable by 0.035 eV than the former.[13] Therefore, in Section IV, we present elastic cross sections for both conformations in order to justify why we will consider only the *trans* isomer for the more computationally expensive multichannel coupling calculations. Furfural, with C_s symmetry, can be considered structurally similar to furan (C_4H_4O), with C_{2v} symmetry, since they only differ by the substitution of a hydrogen atom in furan by a formyl (COH) group in furfural. We can also consider furfural to be similar in structure to tetrahydrofuran (C_4H_8O), although the latter is saturated and therefore does not support π^* shape resonances. Nonetheless we can expect to observe similarities in the scattering cross sections for these related molecules (see Fig. 1). Regarding the low-energy resonance spectra, it is well known that furan has two π^* shape resonances (there are two double bonds on the ring) in the B_1 and A_2 symmetries located at around 2.0 eV and at 3.6 eV, respectively.[15] Furfural would therefore be expected to have three π^* shape resonances in the A'' symmetry, in view of the additional double bond in the formyl group. All these points are considered in Section IV. In Section V, we present calculated elastic and electronically inelastic differential cross sections for the scattering of electrons by furfural for energies up to 50 eV. For a few energies, for elastic and electronically inelastic excitations, we also compare our results with corresponding electron-scattering data independently obtained for furan and tetrahydrofuran (THF) in this section. Finally, in Section VI, we summarize our findings with some conclusions.

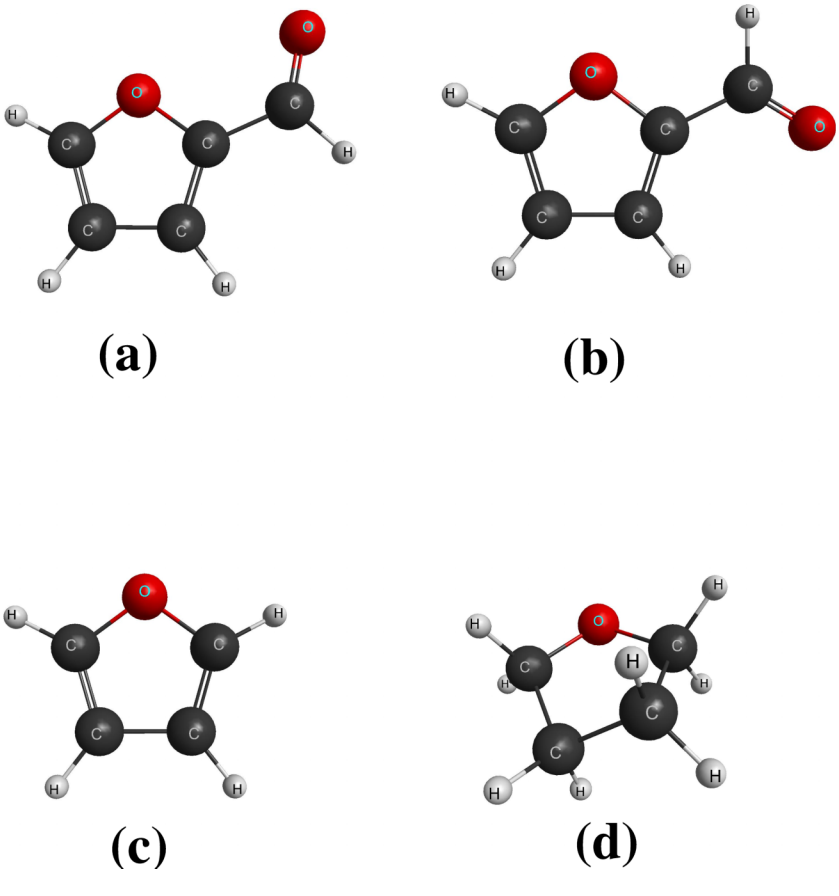

FIG. 1. Geometrical structures of (a) *cis*-furfural, (b) *trans*-furfural, (c) furan, and (d) tetrahydrofuran. These plots were generated with the software MacMolPlt.[14]

II. THEORETICAL METHODS

A. The Schwinger multichannel method with pseudopotentials (SMCPP)

The Schwinger multichannel (SMC)[16] method for electron-molecule scattering is a variational approach specially designed to deal with targets of arbitrary geometries. For this, it uses square integrable basis functions to obtain the scattering amplitudes. The method takes into account important effects such as the electron exchange, the electron-target polarisation interaction and the possibility of flux competition between the elastic and inelastic channels through electronic multichannel coupling. The high computational cost for getting meaningful results, for polyatomic targets, led us to use parallel computing[17] in an implementation that also employs norm-conserving pseudopotentials[18] (SMCPP) and single-excitation configuration interaction techniques for the target description.[19] Since the method has been recently reviewed,[20] here we only give the working expression for the scattering amplitude,

$$f(\mathbf{k}_f,\mathbf{k}_i) = -\frac{1}{2\pi}\sum_{m,n}\langle S_{\mathbf{k}_f}|V|\chi_m\rangle(d^{-1})_{mn}\langle\chi_n|V|S_{\mathbf{k}_i}\rangle, \quad (1)$$

where

$$d_{mn} = \langle\chi_m|\left[\frac{\hat{H}}{N+1} - \frac{\hat{H}P + P\hat{H}}{2} + \frac{PV+VP}{2} - VG_P^{(+)}V\right]|\chi_n\rangle. \quad (2)$$

In the expressions above, P is a projector onto N_{open} energy-allowed target electronic channels, i.e.,

$$P = \sum_{\ell=1}^{N_{open}} |\,\Phi_\ell\rangle\langle\Phi_\ell\,|, \quad (3)$$

with $|\,\Phi_\ell\rangle$ written as a single-excitation configuration-interaction wave function, $G_P^{(+)}$ is the free-particle Green's function projected onto the P space, V is the electron-target interaction potential, $\mathbf{k}_i$ ($\mathbf{k}_f$) is the incoming (outgoing) projectile wave vector, and $\hat{H} = E - H$ is the total energy (ground state energy plus kinetic energy of the incoming electron) minus the Hamiltonian of the $(N+1)$ electrons under the field of the fixed nuclei. The latter is given by $H = H_0 + V$, where H_0 describes the non-interacting electron-molecule system and $S_{\mathbf{k}}$ is a solution of H_0, namely, the product of a plane wave (projectile) and a target state $|\Phi_\ell\rangle$. For the expansion of the variational scattering wave function, the method employs trial basis sets comprising $(N+1)$-particle configuration state functions (CSFs), denoted by $|\chi_m\rangle$, that are built from spin-adapted, anti-symmetrized products of target electronic states and projectile scattering orbitals. The energetically open electronic collision channels are included in the P space, and the dynamical response of the target electrons to the projectile field (correlation-polarisation effects) is accounted for through virtual excitations of the target. In this case, the CSFs are given by

$$|\chi_m\rangle = \mathcal{A}_{N+1}|\Phi_i(1,\ldots,N)\rangle \otimes |\varphi_j(N+1)\rangle, \quad (4)$$

where for $i > 0$, $|\Phi_i\rangle \equiv {}^{(2S+1)}(h_i \to p_i)$ is a singly excited state obtained by promoting one electron to create a hole orbital (h_i) in the ground state $|\Phi_0(1,\ldots,N)\rangle$ and occupy a particle orbital (p_i), with either singlet $(S=0)$ or triplet $(S=1)$ spin coupling, though only $(N+1)$-electron configurations with total spin $S = 1/2$ (doublets) are actually taken into account. If we have N_{open} states in Eq. (3), this level of calculation is called an N_{open}-channel coupling scheme at the static-exchange-plus-polarisation (acronym is N_{open}ch-SEP) approximation. For static-exchange with N_{open} states the acronym is the N_{open}ch-SE approximation. In order to transform the scattering amplitude from the body-fixed frame (the reference frame best suited for carrying out the calculations) to the laboratory-fixed frame (the reference frame where the z-axis is aligned with the direction of incident wave vector, i.e., $\mathbf{k}_i = k_i\hat{\mathbf{z}}$), we expand $\mathbf{k}_f$ in terms of partial waves[21]

$$f(\mathbf{k}_f,\mathbf{k}_i) \equiv \langle\mathbf{k}_f|f|\mathbf{k}_i\rangle = \sum_{\ell=0}^{\ell_{max}}\sum_{m=-\ell}^{\ell}\langle\mathbf{k}_f|\ell m\rangle f(\ell m,\mathbf{k}_i), \quad (5)$$

where $\langle\mathbf{k}_f|\ell m\rangle$ is a spherical harmonic that can be easily converted from the body- to the laboratory-frame and $f(\ell m,\mathbf{k}_i) = \langle\ell m|f|\mathbf{k}_i\rangle$ can be understood as the scattering amplitude of an electron entering the interaction region in a plane-wave $|\mathbf{k}_i\rangle$ and leaving it in a partial wave $|\ell m\rangle$.

For some cases (elastic and dipole-allowed singlet transitions) a Born-closure scheme was used following the same strategy as described in Ref. 4. This closure is obtained from the expression

$$\begin{aligned} f_{\mathrm{LAB}}^{\mathrm{closure}}(\mathbf{k}_f,\mathbf{k}_i) = {} & f_{\mathrm{LAB}}^{\mathrm{FBA}}(\mathbf{k}_f,\mathbf{k}_i) \\ & + \sum_{\ell=0}^{\ell_{max}}\sum_{m=-\ell}^{\ell}\left(f_{\mathrm{LAB}}(\ell m,\mathbf{k}_i) - f_{\mathrm{LAB}}^{\mathrm{FBA}}(\ell m,\mathbf{k}_i)\right) \\ & \times Y_{\ell m}^*(\mathbf{k}_f), \end{aligned} \quad (6)$$

where $f_{\mathrm{LAB}}^{\mathrm{FBA}}$ is the scattering amplitude for the permanent dipole moment potential for the elastic process or for the dipole transition potential for inelastic dipole-allowed processes. Both are obtained in the first Born approximation, in a closed form in the laboratory-frame. The amplitude $f_{\mathrm{LAB}}(\ell m,\mathbf{k}_i)$ is just the $f(\ell m,\mathbf{k}_i)$ of Eq. (5) transformed to this frame.

For the total cross section, we have used the optical theorem directly on the linear representation of the scattering amplitude, given by Eq. (1), i.e.,

$$\sigma_{\mathrm{tot}} = \frac{1}{4\pi}\int d\Omega_{\mathbf{k}_i}\frac{4\pi}{k}\mathrm{Im}f(\mathbf{k}_i,\mathbf{k}_i) = \sum_{n=1}^{N_{open}}\sigma(1\to n), \quad (7)$$

where $\sigma(1 \rightarrow n)$ is the integral cross section for the electronic transition $1 \rightarrow n$. In order to correct the contribution from the low-angular region (important for the elastic transition since some molecules have a non-negligible permanent dipole moment, and also for singlet excitations to dipole-allowed states), we have also calculated the TCS, using the amplitudes obtained from Eq. (6), and the expression

$$\sigma_{\rm tot}^{\rm closure} = \sum_{n=1}^{N_{open}} \sigma^{\rm closure}(1 \rightarrow n), \tag{8}$$

where $\sigma^{\rm closure}(1 \rightarrow n) \neq \sigma(1 \rightarrow n)$ only for the above mentioned transitions.

The SMC method does not take the ionisation channel into account. In order to obtain the total scattering cross section we need to compute the elastic and inelastic cross sections and the total ionisation cross section. To estimate the total ionisation cross section we have used the binary-encounter-Bethe (BEB) model.[22] The BEB model results in a simple expression for the ionisation cross section per molecular orbital, given by

$$\sigma_{BEB}(T) = \frac{S}{t+u+1}\left[\frac{\ln t}{2}\left(1-\frac{1}{t^2}\right)+1-\frac{1}{t}-\frac{\ln t}{t+1}\right]. \tag{9}$$

In the above equation, T is the incident electron energy, $t = T/B$ and $u = U/B$ are normalized energies, B and U being the orbital binding and the electron kinetic energy, respectively, $S = 4\pi a_0^2 N_{\rm occ} R^2/B^2$ where $N_{\rm occ}$ is the orbital occupation number, $a_0 = 0.5292$ Å, and $R = 13.61$ eV. To obtain the total ionisation cross section one needs to sum $\sigma_{BEB}(T)$ over the molecular orbitals satisfying $T > B$. The resulting total cross sections typically agree with experiment to within 5%-15% for many different molecules and for incident energies ranging from the first ionisation threshold to several keV.[23,24]

B. Independent atom method with screening corrected additivity rule (IAM-SCAR)

The IAM-SCAR method has had significant use in calculating electron scattering cross sections for a wide variety of molecular targets (see, e.g., Refs. 25–30), and over a broad energy (E_0) range (typically ~1–5000 eV). As a consequence, we only précis the key points of that approach here.

The first subjects of our computations are the individual atoms that form furfural, namely, carbon (C), oxygen (O), and hydrogen (H). The atomic optical model (OM) is based on a potential scattering approach, where the local complex potential $V(r)$ is given by

$$V(r) = V_{\rm s}(r) + V_{\rm ex}(r) + V_{\rm p}(r) + iV_{\rm a}(r). \tag{10}$$

In the above equation $V_{\rm s}(r)$ is the standard Hartree potential of the target, $V_{\rm ex}(r)$ represents the exchange interaction of Riley and Truhlar,[31] $V_{\rm p}(r)$ is the polarisation potential of Zhang *et al.*,[32] and $V_{\rm a}(r)$ is the imaginary absorption potential of Staszewska *et al.*[33] Due to the last term in Eq. (10), the OM potential approach yields a complex phase shift. This allows for the calculation of the DCSs and ICSs for elastic and inelastic (taken to mean all the excited electronic states and ionisation processes combined together) scattering, as well as the TCS as the sum of those ICSs, for each atom.

We subsequently calculate the electron-$C_5H_4O_2$ cross sections by applying the additivity rule (AR) to the OM results of each atom. In that approach, the molecular scattering amplitude stems from the sum of all the relevant atomic amplitudes, including the phase coefficients, which gives the elastic DCSs for furfural. Elastic ICSs can then be determined by integrating those DCSs. The sum of the elastic and absorption ICSs (for all inelastic processes except rotations and vibrations) then gives the molecular TCS. However the AR does not account for the target molecular structure, so that it is only applicable when the incident electrons are so fast that they effectively "see" the target molecule as a sum of the individual atoms (typically above ~100 eV). To try and overcome this limitation, Blanco and García[34,35] introduced the screening corrected AR (SCAR) method which employs some screening coefficients to account for the geometry of the molecule (atomic positions and bond lengths). The IAM-SCAR method as described does not account for rotational and vibrational excitations. However, for polar molecules such as $C_5H_4O_2$, additional dipole-induced excitation cross sections can be computed using the approach of Jain.[36] In that method, rotational excitation DCSs and ICSs for a free electric dipole are calculated within the framework of the first Born approximation. Those results can now be incorporated into our IAM-SCAR results in an incoherent way, just by adding up the cross sections as independent channels. We call the cross sections that result from this latter process as "IAM-SCAR+rotations." There is a body of evidence that suggests that the IAM-SCAR approach for non-polar molecules and IAM-SCAR+rotations method for polar species[25–30] provides a fair description of the measured cross sections down to $E_0 = 20$ eV. However, there are also some examples[37–39] where the comparison between these two approaches and the measured cross sections is only reasonable at energies above ~50 eV. As a result of the latter observation, at least in part, Blanco and García[40] recently introduced an interference term (I) to help describe that the collision dynamics involves scattering from multiple centres. Full details can be found in Ref. 40, we simply note that the method applied here is called IAM-SCAR+I. Therefore, one of the rationales of the present investigation was to test the efficacy of the new IAM-SCAR+I results against corresponding results from our fully *ab initio* SMCPP at the N_{open}ch-SEP and N_{open}ch-SE level computations, at representative energies of 50 eV and below.

III. COMPUTATIONAL PROCEDURES FOR THE PRESENT APPLICATION OF THE SMCPP METHOD

Although the convergence trend with respect to angular momentum is not shown here, all SMCPP differential cross sections in this paper, over the entire energy range (5-50 eV), are numerically converged with $\ell_{max} = 10$ (including for 50 eV), if combined with a quadrature point distribution, using a 26 Gauss-Legendre scheme for $0 \leq \theta_i \leq \pi$ and 52 points for

$0 \le \phi_i \le 2\pi$, to describe $\mathbf{k}_i(\theta_i, \phi_i)$ in spherical coordinates. As in any multi-center expansion, we have contributions from high partial waves in the scattering orbitals due to Cartesian Gaussians (CGs) of s, p, and d types on the two oxygen atoms and on each center for the carbon atoms. On the hydrogen atoms, we have only CG functions of s and p types. As discussed in our previous applications,[20] the limitation on the CG types makes the description of the high partial waves more difficult, but the large number of CG centers compensates this truncation, resulting in good convergence for the elastic and inelastic differential cross sections. We have also used pseudopotentials for the carbon and oxygen atoms. This strategy allows a reduction in the number of Cartesian Gaussian functions, since it is not necessary to consider those involved in the description of all 1s orbitals of these atoms.

The ground state of the furfural *trans* conformation was obtained in the Hartree-Fock approximation, using 241 CG functions (5s, 5p, 2d on each C and O atom, 4s/3s on three H atoms and 6s/5s, 1p on the H atom of the aldehyde functional group), giving a permanent dipole moment of 4.85 D (3.94 D) for the *cis* (*trans*) isomer, against the experimental value of 3.97 D (3.23 D).[41] We first ran a full single excitation configuration interaction (FSCI) which gave 4014 states, with 32 (53) of them below 9 eV (10 eV) (from the ground state). Using a mixture of hole orbitals, we obtained a set of improved virtual orbitals capable of reproducing 26 of those states below 9 eV (30 below 10 eV) using only 31 hole-particle pairs. This procedure defined the minimum orbital basis for single-excitation configuration interaction (MOB-SCI)[19] of the present application. The 31 hole-particle pairs give rise to 31 triplets and 31 singlets states (see Table I of Ferreira da Silva *et al.*[11]). In this description, 31 electronic states are open at 10 eV (31ch-SEP approximation), 53 electronic channels are open at 20 eV (53ch-SEP approximation), and all 63 electronic channels are open at 30, 40, and 50 eV (63ch-SE approximation, no additional closed channels for polarisation effects). The present application for furfural uses therefore a projector P containing up to 63 electronic states. For energies above 26 eV, this is our most sophisticated (with the largest channel coupling) application of the SMCPP method to date. Although promising, it is important to point out that the present FSCI calculation, with 241 CG functions, generated 32 electronic excited states below 9 eV, 53 below 10 eV, 102 below 12 eV, 263 below 15 eV, and 688 excited states below 20 eV. This high density molecular spectra, due to a combination of high density Rydberg states, increase as we augment the CG basis set. Our MOB-SCI calculation includes most of the states (26 of the 32 FSCI states) below 9 eV but the computationally needed truncation generated important convergence consequences, as we will discuss in Secs. IV and V. Although not accounted for in the scattering calculation, the present Hartree-Fock approximation for the ground state of furfural shows the first 3 ionisation potentials (Koopmans theorem) at 9.2, 11.4, and 12.0 eV, respectively. Thus our MOB-SCI calculation is almost the complete calculation using all open channels up to 9 eV. Note, however, that a "complete" calculation using all possible open channels up to 12 eV would have the ground state plus 102 discrete excited states plus 3 ionisation channels.

For the previously discussed BEB model, the ionisation, B, and kinetic, U, orbital energies needed in Eq. (9) were obtained in a Hartree-Fock calculation with the aug-cc-pVDZ basis set at the optimized geometry at the MP2 level with the same basis set, using GAMESS.[42] We have used a single channel ionisation potential of the *trans* furfural isomer at 9.30 eV, in good agreement with the experimental value of 9.22 eV.[43,44]

IV. RELATIVE ABUNDANCE AND LOW-ENERGY SCATTERING

A few properties of the *cis* and *trans* isomers were investigated with density functional theory (DFT) employing the hybrid functional B3LYP and the correlation-consistent aug-cc-pVDZ basis set, as implemented in the GAMESS package.[42] The calculated electric dipole moment of the *cis* (*trans*) isomer was 4.45 D (3.79 D), somewhat overestimated with respect to the experimental value of 3.97 D (3.23 D).[41] The dipole moment magnitudes strongly suggest the existence of dipole bound states for both isomers, but these were not investigated.

The calculated relative energy of the *cis* isomer to the most stable *trans* isomer was 29 meV, in good agreement with the experimental result of 35 meV.[13] At the temperature of our typical experiments,[11,12,44] ~60 °C, the Boltzmann factor between the isomers is 0.32, such that the relative population (*cis*-to-*trans*) would be around 1:3. In view of the significant computational effort required by the 63-channel scattering calculations, we only address the *trans* isomer, accounting for ≈80% of the gas-phase population. The most significant difference between the isomers is related to the larger dipole moment of the *cis* form. However, the dipolar potential would only be expected to impact the elastic DCSs at lower scattering angles (<20°), and hence the magnitude of the corresponding elastic ICSs should be similar for both isomers. An upper bound for the difference in magnitude of the ICSs at low energies can be obtained from a pure dipole scattering model, i.e., $\sigma_{cis}/\sigma_{trans} = (D_{cis}/D_{trans})^2 \approx 1.4$. However, based on previous results for the D-glucose monomers,[4] we expect smaller discrepancies above 1 eV. Finally, we also report MTCSs which have significantly smaller contributions from the forward scattering arising from the dipolar interaction. These MTCSs are particularly important when seeking to model the transport of charged particles under the influence of an applied electric field.[45]

At lower energies, SMC single-channel elastic scattering calculations were carried out for both isomers. We employed the static-exchange (SE) approximation that neglects the dynamical response of the target electrons to the projectile (no target excitations in Eq. (4)), and the SE plus polarisation (SEP) approximation that accounts for correlation-polarisation effects, according to Eq. (4). The cross sections were symmetry-decomposed into the A' and A'' components of the C_s group to highlight the resonance signatures and reduce the computational effort. The A'' CSF space was built according to the procedure of Ref. 46. A set of modified virtual orbitals (MVOs)[47] was obtained from a cationic Fock

operator with charge +4, and the three lowest-lying A'' MVOs were used as scattering orbitals (see Eq. (4)). To expand the scattering trial function, all symmetry-preserving target excitations with both singlet and triplet spin couplings were taken into account. For the A' symmetry, where no long-lived resonances are found, we employed the 40 lowest-lying MVOs as both scattering and particle orbitals, including all symmetry-allowed target excitations with both singlet and triplet spin couplings.

As previously mentioned, a rich spectrum of π^* anion states can be anticipated for the furfural isomers. The cross sections obtained in the SE approximation (not shown here) indeed suggest three π^* resonances, hereafter labelled π_1^*, π_2^*, and π_3^* from the lowest- to the highest-lying. However, the A'' component of the ICS obtained in the SEP approximation, shown in Fig. 2, only displays two resonances at around 2.16 eV (1.93 eV) and 4.0 eV (4.2 eV) for the *cis* (*trans*) isomer (the higher-lying peaks are pseudoresonances that arise because energetically open channels are treated as closed in the single-channel scattering calculations). The diagonalization of the scattering Hamiltonian in the CSF space indicates that the π_1^* state is vertically bound for both furfural forms, with binding energies $\lesssim$0.1 eV. As discussed elsewhere,[48] we cannot be certain about the existence of these bound states in view of the limited precision of the calculations (they could actually be extremely low-lying resonances, just above 0 eV). Nonetheless, the bound state character of the π_1^* valence state was also suggested by the DFT/B3LYP/aug-cc-pVDZ method described above. The calculated binding energy was 0.045 eV (0.081 eV) for the *cis* (*trans*) isomer.

To gain further insight into the shape resonances we obtained, the HF canonical virtual orbitals (VOs) employing the compact basis sets 6-31G(d) are also shown in Fig. 2. The VO energies can also be used to estimate the vertical attachment energies (VAEs) employing the empirical scaling relation of Staley and Strnad[49] (to our knowledge, there are no experimental data on the resonance spectra of the furfural isomers). Denoting bound and resonance states by negative and positive energies, respectively, the π_1^*, π_2^*, and π_3^* VAE estimates are, respectively, −0.053 eV (−0.063 eV), 1.97 eV (1.89 eV), and 3.32 eV (3.44 eV) for the *cis* (*trans*) isomers. These semiempirical VAEs also support the existence of bound states (π_1^*) and are in good agreement with the SMC scattering results. The worst agreement is for the π_3^* resonance, as would be expected in view of its mixed shape and core-excited character.[50,51] Note that the three π^* anion states have amplitudes delocalized over the ring and the formyl group. The bound π_1^* anion seems to be stabilized by the bonding character of the C–C bond between the ring and the formyl group.

Narrow σ^* shape resonances would not be expected for the furfural isomers. Indeed, the A' partial ICS, shown in Fig. 3, does not show evidence of such anion states (inspection of the four lowest-lying compact VOs of both isomers suggests either a dipole character or a σ^*_{CH} character). The ICS magnitudes of the isomers are fairly close in value above 1 eV, although they have not been corrected to account for the dipolar potential contribution to the higher partial waves. There is a broad structure around 6 eV, which is more evident for the *cis* isomer. However, in view of the number of energetically open channels around 6 eV (see Table I) we would not rely on the single-channel approximation at this energy.

Our present results show that all resonant structures below 10 eV are present in both *trans* and *cis* conformations. Our earlier results of Ref. 11 showed that the 1ch-SEP elastic cross sections for the *cis* and *trans* conformations are quite similar to each other for the 10–50 eV energy region. Besides, for the majority of electronic states obtained for the *trans* conformation there is a counterpart state (lying near to it) for the *cis* conformation. Therefore, considering that the gas mixture contains about 80% of the *trans* and about 20% of

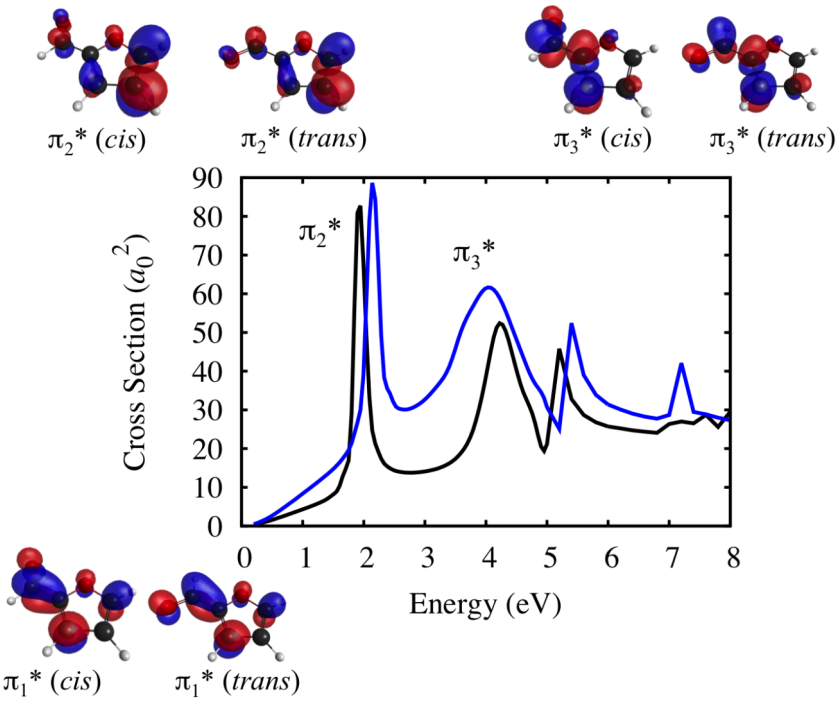

FIG. 2. A'' partial integral cross section for elastic electron scattering by the *cis* (blue line) and *trans* (black line) furfural isomers. The calculations were carried out with the SMC method in the single-channel SEP approximation (see text). The $\pi^*_{2,3}$ shape resonances are indicated in the panel, while the lowest-lying π_1^* anion is vertically bound, according to the present computations. The lowest-lying A'' virtual orbitals obtained with the compact 6-31G(d) basis set are also shown and labelled as π_1^* (bottom left), π_2^* (top left), and π_3^* (top right).

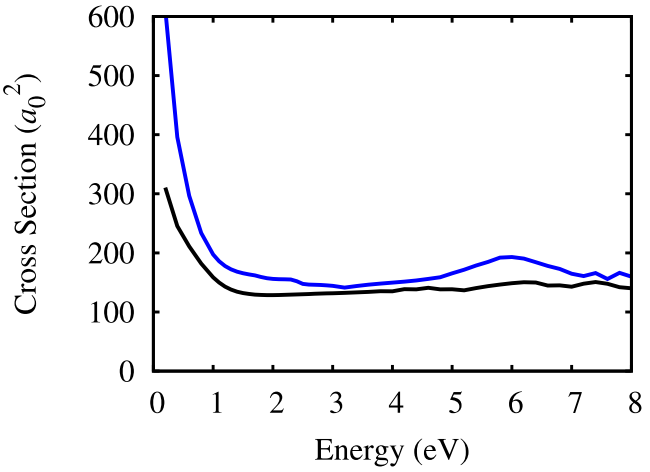

FIG. 3. A' partial integral cross section for elastic electron scattering by the *cis* (blue line) and *trans* (black line) furfural isomers. The partial cross sections were not corrected to account for the contribution of the dipolar potential to the higher partial waves (see text).

the *cis* conformation, we feel comfortable to assume that we can obtain reasonable multichannel scattering results for the furfural molecule by only calculating the scattering amplitudes for the *trans* conformation.

V. RESULTS AND DISCUSSION

In Figs. 4–6, we show how the inclusion of multichannel coupling impacts on our calculated elastic integral-, momentum transfer-, and differential cross sections. In order to do this, we compare the cross sections obtained according to the different channel coupling schemes, starting from the 1ch-SEP approximation, where only the elastic channel is open, to the 63ch-SE approximation, which is our most complete calculation having 63 open channels. The results presented in Fig. 4 start at different energies due to distinct thresholds used in each calculation, as indicated in Table I. Fig. 4 displays a systematic decrease in the magnitude of the integral and momentum transfer cross sections as more channels became energetically allowed. Indeed, the main effect of multichannel coupling is to allow flux from the elastic channel to go to the inelastic channels, which explains the decrease in magnitude

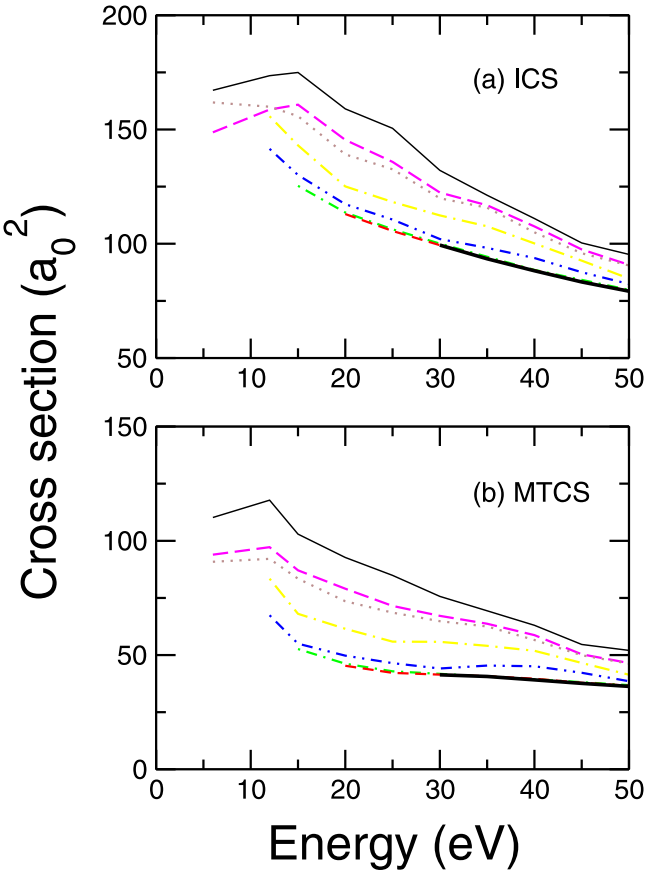

FIG. 4. Influence of the multichannel coupling effects (a) on the elastic integral (ICS) and (b) on the momentum transfer (MTCS) cross sections of furfural. The results shown here were obtained according to the 1ch-SEP up to the 63ch-SE levels of approximation, depending on the energy considered (see text for details). Thin solid (black) line: 1ch-SEP; long-dashed (magenta) line: 4ch-SEP; dotted (brown) line: 6ch-SEP; long dashed-dotted (yellow) line: 7ch-SEP; dashed-dotted-dotted (blue) line: 31ch-SEP; short dashed-dotted (green) line: 53ch-SEP; short dashed (red) line: 57ch-SEP; full solid (black) line: 63ch-SE approximation.

in the integral and momentum transfer cross sections as more channels open up. There is a large drop in the cross section magnitude in going from the 1ch-SEP to the 4ch-SEP, a small one from the 4ch-SEP to the 6ch-SEP, another big drop in the magnitude from the 7ch-SEP to the 31ch-SEP, and a small

TABLE I. Summary of the calculated and experimental excitation energies below 10 eV for furfural from Ref. 11. The MOB-SCI calculation aimed to reproduce all 30 states of the FSCI calculation lying below 10 eV. These are 7 triplet and 5 singlet states listed below. The remaining MOB-SCI below 10 eV are 11 singlet states opening up at 6.64, 7.37, 7.51, 7.76, 8.09, 8.27, 8.30, 8.37, 8.80, 9.05, and 9.14 eV and 13 triplet states opening up at 6.51, 6.77, 7.26, 7.46, 7.85, 7.97, 8.14, 8.18, 8.28, 8.64, 8.96, 9.13, and 9.95 eV. The MOB-SCI also contains 32 less precise states (pseudostates), 18 singlets, and 14 triplets, lying between 10 and 25.2 eV.

			Dipole transition	Energy (eV)		
	Expt. band	Symmetry	in Debye	FSCI	MOB-SCI	TD-DFT
Triplet	Band 1 (2.7-4.4 eV)	A'	...	2.60	3.00	2.82
	Band 1 (2.7-4.4 eV)	A''	...	4.03	4.35	3.11
	Band 2 (4.4-5.4 eV)	A'	...	4.46	4.73	4.53
	Band 2 (4.4-5.4 eV)	A'	...	5.18	5.47	5.01
Singlet	Band 1 (2.7-4.4 eV)	A''	0.16	4.72	4.97	3.65
	Band 2 (4.4-5.4 eV)	A''	4.80	5.46	6.30	4.79

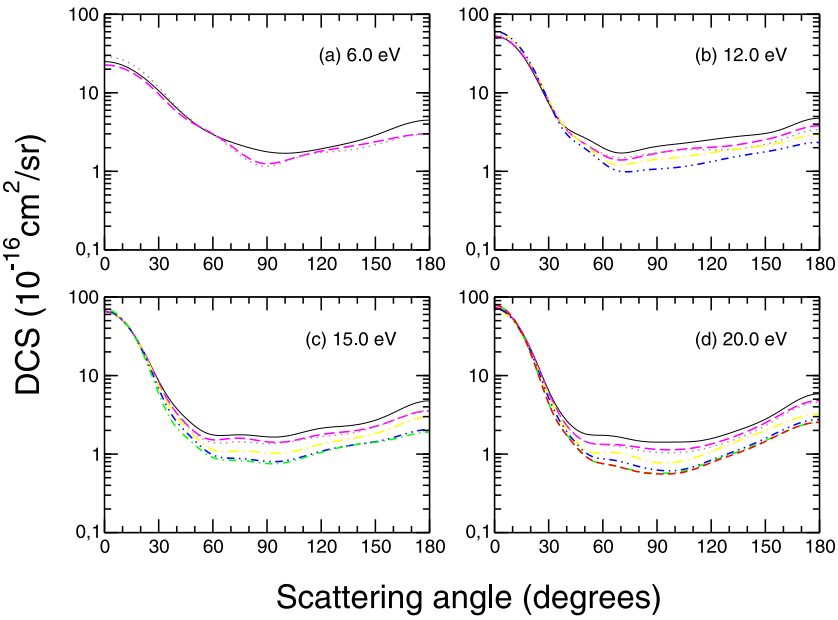

FIG. 5. Influence of the multichannel coupling effects on the elastic differential cross sections of furfural for (a) 6.0 eV, (b) 12.0 eV, (c) 15.0 eV, and (d) 20.0 eV electron impact energies. Thin solid (black) line: 1ch-SEP; long-dashed (magenta) line: 4ch-SEP; dotted (brown) line: 6ch-SEP; long dashed-dotted (yellow) line: 7ch-SEP; dashed-dotted-dotted (blue) line: 31ch-SEP; short dashed-dotted (green) line: 53ch-SEP; short dashed (red) line: 57ch-SEP approximation.

drop from the 31ch-SEP to the 53ch-SEP results. The cross sections obtained in the 53ch-SEP, 57ch-SEP, and 63ch-SE approximations agree very well with each other, suggesting that the results, at least with respect to the electronic inelastic channels (since there are no ionisation channels included in these calculations), are converged up to 50 eV. The same behavior presented by the integral and momentum transfer cross sections is observed in the elastic differential cross sections, shown in Fig. 5, for energies at 6, 12, 15, and 20 eV, and in Fig. 6, for energies of 25, 30, 40, and 50 eV. They also clearly decrease in magnitude, particularly for scattered electron angles greater than 20°, as more channels are included in the calculations. Except at 6 eV, where there are only 4 channels open, there is a considerable difference in magnitude between the 1ch-SEP results and the best calculation (with all channels open) for the other energies.

Now, in Fig. 7, we compare our integral-, momentum transfer-, and total cross sections obtained by the SMCPP method at the 1ch-SEP and up to 63ch-SE levels of approximation and by the IAM-SCAR+I method with experimental[15,53–56,59,60] and other theoretical[25,52,57,58] results for furan and THF molecules, that as mentioned before can be considered as being structurally similar to furfural. The curves presented in this figure as a full solid black line contain contributions from calculations starting with 6ch-SEP up to the 63ch-SE (considering the different thresholds) and represent our most complete calculation for energies from 5 to 50 eV. The SMCPP results obtained at the 1ch-SEP level of approximation (thin solid black line) are bigger in magnitude than all the other results for furan and THF shown in this figure, while the integral cross sections given by the full solid black line (SMCPP results obtained within the 6ch-SEP up to

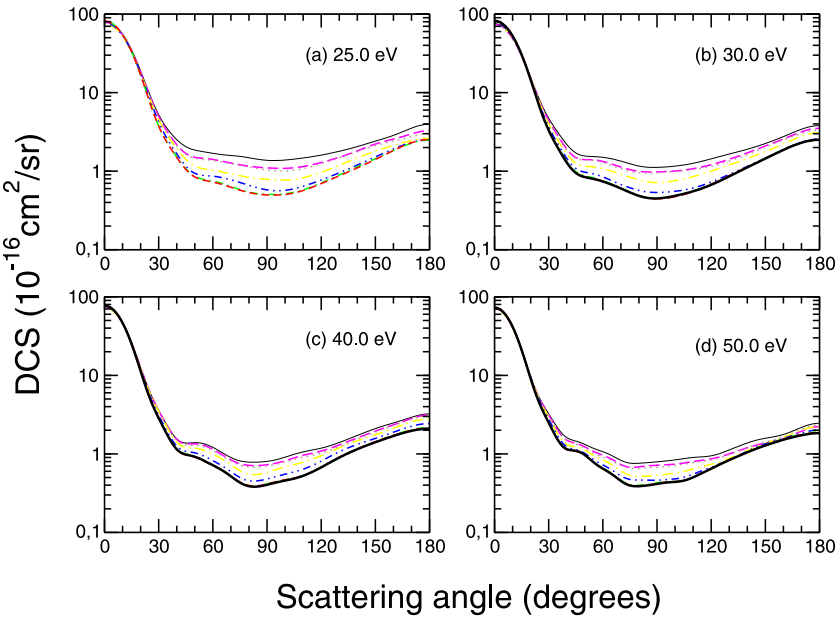

FIG. 6. Influence of the multichannel coupling effects on the elastic differential cross sections of furfural for (a) 25.0 eV, (b) 30.0 eV, (c) 40.0 eV, and (d) 50.0 eV electron impact energies. Thin solid (black) line: 1ch-SEP; long-dashed (magenta) line: 4ch-SEP; dotted (brown) line: 6ch-SEP; long dashed-dotted (yellow) line: 7ch-SEP; dashed-dotted-dotted (blue) line: 31ch-SEP; short dashed-dotted (green) line: 53ch-SEP; short dashed (red) line: 57ch-SEP; full solid (black) line: 63ch-SE approximation.

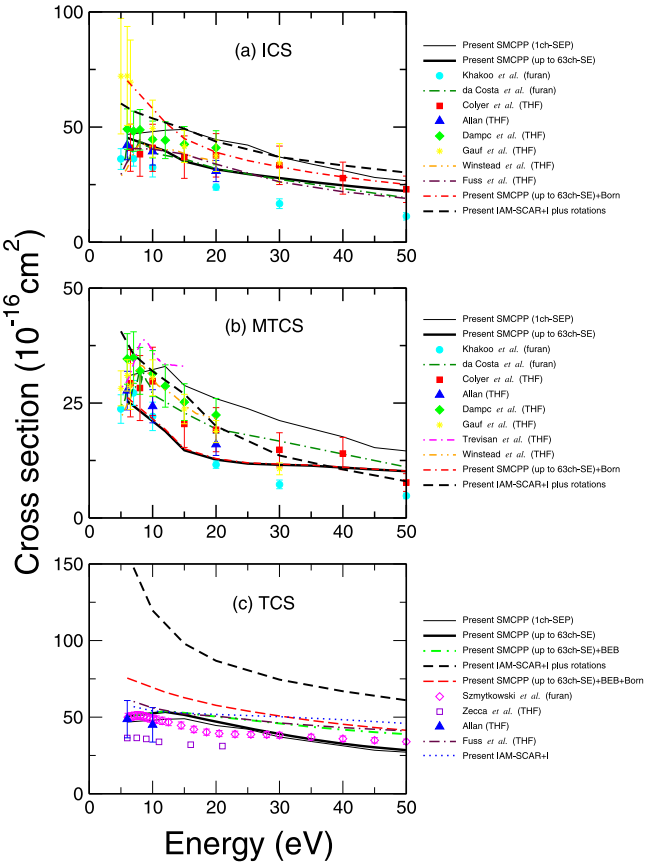

FIG. 7. Elastic (a) integral (ICS), (b) momentum transfer (MTCS), and (c) total (TCS) cross sections of furfural. The SMCPP results shown here were obtained according to the 6ch-SEP up to the 63ch-SE levels of approximation, depending on the energy considered (see text for details). Thin solid (black) line: SMCPP 1ch-SEP; full solid (black) line: SMCPP from 6ch-SEP up to 63ch-SE approximations (referred as SMCPP (up to 63ch-SE) in the legends); dashed-dashed-dotted (red) solid line: SMCPP (up to 63ch-SE)+Born ICS and MTCS (see text for details); full dashed-dotted green line: SMCPP (up to 63ch-SE) TCS plus total BEB ionisation cross section (see text for details); full long dashed (red) line: SMCPP (up to 63ch-SE)+Born TCS plus total BEB ionisation cross section (see text for details); full dashed (black) line: IAM-SCAR+I plus rotations; full dotted (blue) line: IAM-SCAR+I (see text for details); full (cyan) circles: experiments for furan of Ref. 15; long dashed-dotted (dark green) line: SMCPP up to 9ch-SEP results for furan of Ref. 52; full (red) squares: experiments for THF of Ref. 53; full (green) diamonds: experiments for THF of Ref. 54; full (blue) up triangles: experiments for THF of Ref. 55; (yellow) stars: experiments for THF of Ref. 56; dashed-dotted (magenta) line: complex-Kohn elastic results for THF of Ref. 57; dashed-dotted-dotted (orange) line: SMC elastic results for THF of Ref. 58; long dashed-dotted (maroon) line: IAM-SCAR results for THF of Ref. 25; open (magenta) diamonds: experiments for furan of Ref. 59; open (violet) squares: experiments for THF of Ref. 60.

63ch-SE levels of approximation) and by the full dashed black line (IAM-SCAR+I plus rotations) are within the experimental error bars, and with about the same magnitude as the theoretical results for the furan and THF molecules. Such an outcome is not surprising since all these molecules are comparable in size. The SMCPP calculation (with and without closure) corresponds to rotationally summed cross sections (RSCSs), considering the molecule initially in the ground state and being excited to all rotational levels allowed by the angular momentum coupling. The IAM-SCAR+I approximation, however, does not consider the dipole interaction, so that only pure (orientation averaged) elastic DCS are calculated. On the other hand, the IAM-SCAR+I plus rotations calculation, which includes the dipole interactions through a first Born approximation approach, takes into account that the molecular gas is at room temperature. The temperature only affects the very low angular region of the DCS, but this can have a strong effect on the ICS. Therefore, in terms of DCS comparisons: the SMCPP and IAM-SCAR+I results can be compared, but excluding the smaller angles of the DCS results, and the SMCPP+Born and IAM-SCAR+I plus rotations results should be compared because both give a full treatment of the dipole interaction, although here again at angles too close to zero degrees differences are expected due to the temperature effect (initial rotational states in the IAM-SCAR+I plus rotations approach are due to a Boltzmann distribution of levels). It is worth noting here that for ICS the temperature effect has a greater influence, and so for the ICS it is not expected that a valid comparison between results from these two approximations might be made. We also include in the bottom panel of Fig. 7, our total cross sections obtained by the optical theorem as given by Eq. (7) summed to the ionisation cross section contribution given by Eq. (9) (dotted-dashed green line). Similar to observations in phenol, the SMCPP (up to 63ch-SE)+BEB TCS agrees well with the experimental data for furan and THF. However, there is a significant discrepancy between our SMCPP (up to 63ch-SE)+BEB TCS and our IAM-SCAR+I plus rotations TCS which we believe might be indicative of how the two approaches differently address dipolar scattering. In order to assess the impact due to the dipole potential contribution (since furfural has a large permanent dipole moment) on the SMCPP results for integral, momentum transfer and total cross sections we have used the Born-closure procedure to include the contribution of higher partial waves, as described in Eqs. (6) and (8). This clearly brings the SMCPP and IAM-SCAR results into somewhat better accord, although an important discrepancy between them remains. Clearly some experimental results would be useful in trying to resolve this issue. Note that such experiments will always suffer from what is known as the "forward angle scattering effect,"[8] and so to give the reader an idea for what an electron-furfural TCS might roughly look like in Fig. 7(c) we also plot the IAM-SCAR+I total cross section with rotations excluded (full dotted blue line). Figs. 8 and 9 compare the present computed differential cross sections with experimental[15,53–56,61–64] and theoretical[25,52,57,58] results for furan and THF. In Fig. 8 we show our results at 6 eV, with a 6ch-SEP calculation, at 12 eV, with a 31ch-SEP result, at 15 eV, with a 53ch-SEP computation, and at 20 eV, with a 57ch-SEP. The DCSs of furfural follow the shape of the DCSs of furan and THF, but with a somewhat different magnitude. At higher energies the agreement improves, as shown in Fig. 9, where we present our results at 25 eV, with a 57ch-SEP, and at 30, 40, and 50 eV, with a 63ch-SE calculation. The good agreement between the DCSs of furfural, furan, and THF, especially at 40 and 50 eV, suggests that at energies high enough these molecules present similar DCSs for the elastic electron scattering process. Our SMCPP+Born DCSs agree well with the IAM-SCAR+I plus rotations results, especially for higher

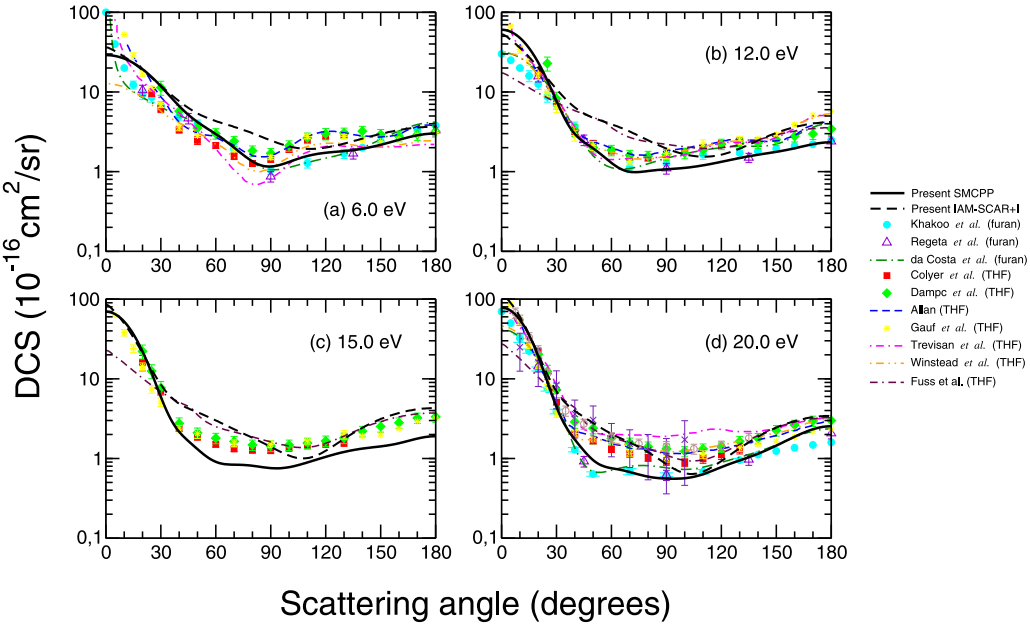

FIG. 8. Elastic differential cross sections of furfural for (a) 6.0 eV, (b) 12.0 eV, (c) 15.0 eV, and (d) 20.0 eV electron impact energies. Full solid (black) line: SMCPP up to 63ch-SE results; full dashed (black) line: IAM-SCAR+I plus rotations at the energies of 7.0, 10.0, 15.0, and 20.0 eV; full (cyan) circles: experiments for furan of Ref. 15; open (violet) up triangles: experiments for furan of Ref. 61; long dashed-dotted (dark green) line: SMCPP up to 9ch-SEP results for furan of Ref. 52; (indigo) crosses: experiments for THF of Ref. 62; full (red) squares: experiments for THF of Ref. 53; full (green) diamonds: experiments for THF of Ref. 54; dashed (blue) line: experiments for THF of Ref. 55; (yellow) stars: experiments for THF of Ref. 56; open (brown) circles: experiments for THF of Ref. 63; dashed-dotted (magenta) line: complex-Kohn elastic results for THF of Ref. 57; dashed-dotted-dotted (orange) line: SMC elastic results for THF of Ref. 58; long dashed-dotted (maroon) line: IAM-SCAR results for THF of Ref. 25.

energies as expected. These results give us real confidence in using our present SMCPP elastic DCSs to undertake our inelastic normalizations in our other furfural experimental studies.[12,65]

Basically, all observations from the analysis of the elastic cross sections are also applicable to the DCSs for the electronically inelastic scattering of electrons by furfural. Representative results involving the transitions from the ground state to the first excited triplet, the third excited triplet, and the first excited singlet states are presented in Figs. 10 and 11, Figs. 12 and 13, and Figs. 14 and 15, respectively. In all transitions considered in the present study (even those not shown here) we found that the magnitude of the DCSs decreases as long as more channels were included in the calculation. For energies from 12 eV to 50 eV, especially at the higher ones, the biggest drop in the magnitude of cross sections occurs when going from the 7ch-SEP to the 31ch-SEP level of approximation. Here it is important to note that at the 31ch-SEP level of approximation all physical states obtained according to the MOB-SCI strategy become energetically allowed and, therefore, were included in the calculation. Once again, it is observed that the cross section results obtained according to the 53ch-SEP, 57ch-SEP, and 63ch-SE levels of approximation are quite similar to each other. But in contrast to the elastic DCSs, comparison with the experimental data for the electronic excitation from the ground

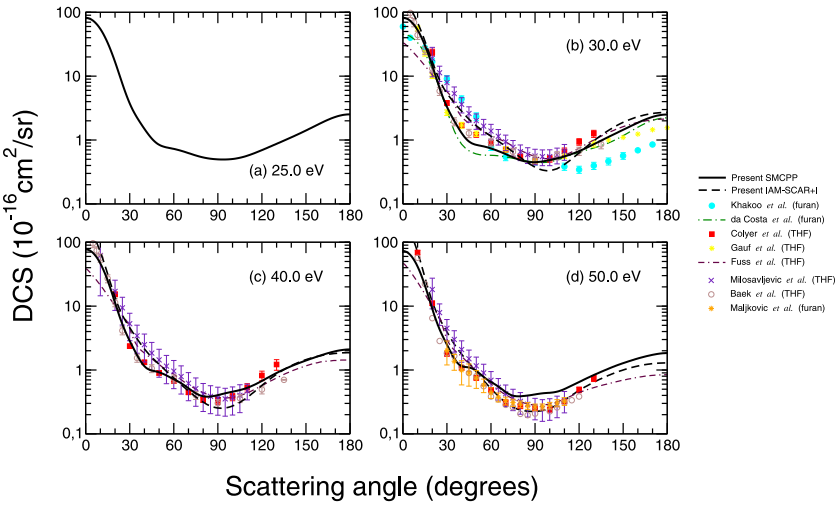

FIG. 9. Elastic differential cross sections of furfural for (a) 25.0 eV, (b) 30.0 eV, (c) 40.0 eV, and (d) 50.0 eV electron impact energies with the same legend definitions as in Fig. 8, except for (orange) stars: experiments for furan of Ref. 64.

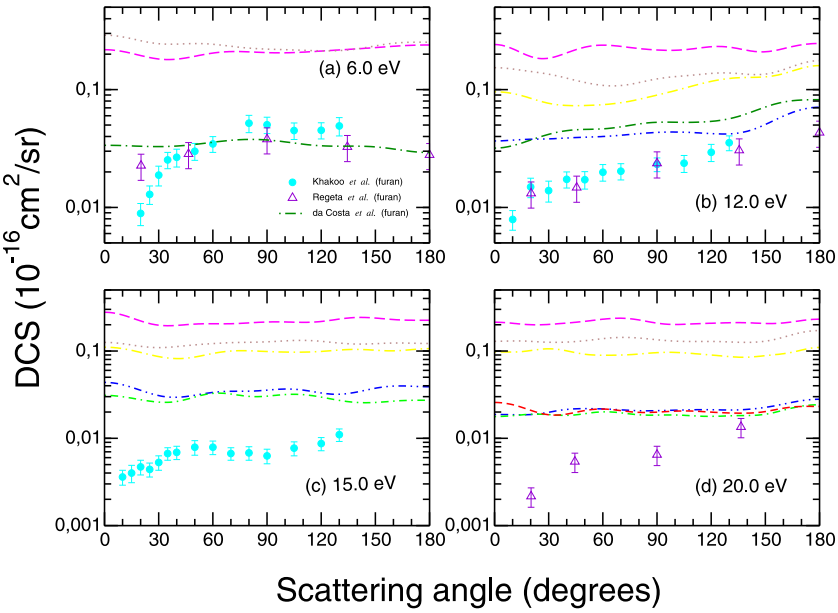

FIG. 10. Influence of the multichannel coupling effects on the electronically inelastic differential cross sections for the first triplet state of furfural for (a) 6.0 eV, (b) 12.0 eV, (c) 15.0 eV, and (d) 20.0 eV electron impact energies with the same legend definitions as in Fig. 5, except for full (cyan) circles: experiments for furan of Ref. 15 at the energies of 6.0, 10.0, and 15.0 eV; open (violet) up triangles: experiments for furan of Ref. 61 at the energies of 6.6, 10.0, and 20.0 eV, long dashed-dotted (dark green) line: SMCPP up to 9ch-SEP results for furan of Ref. 52.

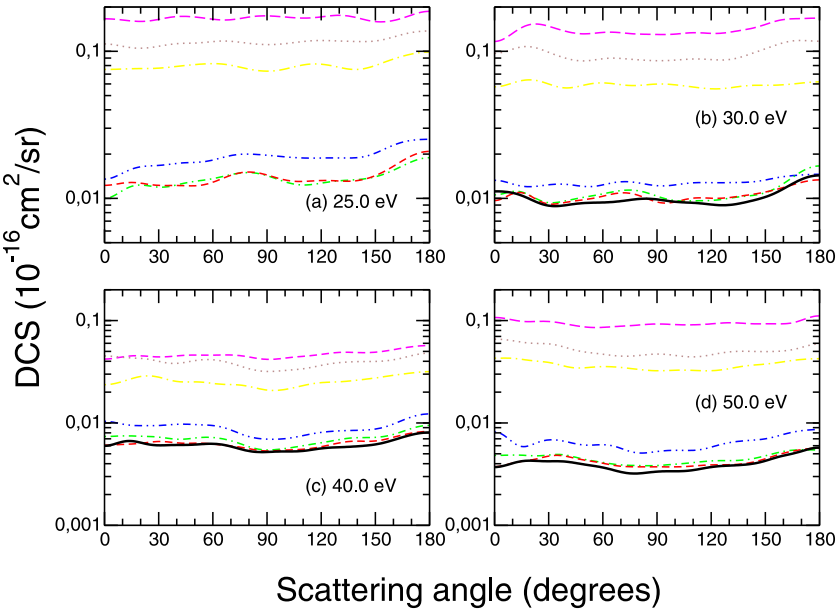

FIG. 11. Influence of the multichannel coupling effects on the electronically inelastic differential cross sections for the first triplet state of furfural for (a) 25.0 eV, (b) 30.0 eV, (c) 40.0 eV, and (d) 50.0 eV electron impact energies with the same legend definitions as in Fig. 6.

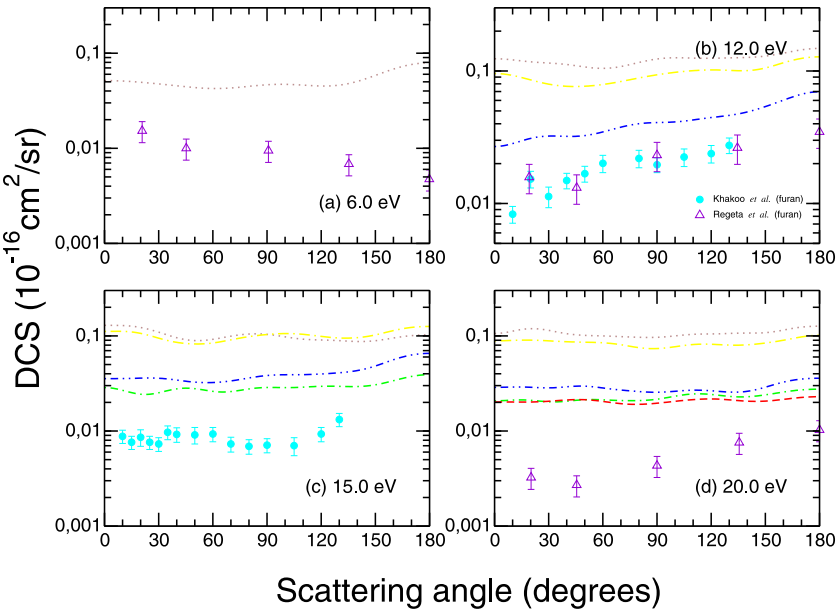

FIG. 12. Influence of the multichannel coupling effects on the electronically inelastic differential cross sections for the third triplet state of furfural for (a) 6.0 eV, (b) 12.0 eV, (c) 15.0 eV, and (d) 20.0 eV electron impact energies with the same legend definitions as in Fig. 5, except for full (cyan) circles: experiments for furan of Ref. 15 at the energies of 10.0 and 15.0 eV; open (violet) up triangles: experiments for furan of Ref. 61 at the energies of 6.6, 10.0, and 20.0 eV, long dashed-dotted (dark green) line: SMCPP up to 9ch-SEP results for furan of Ref. 52.

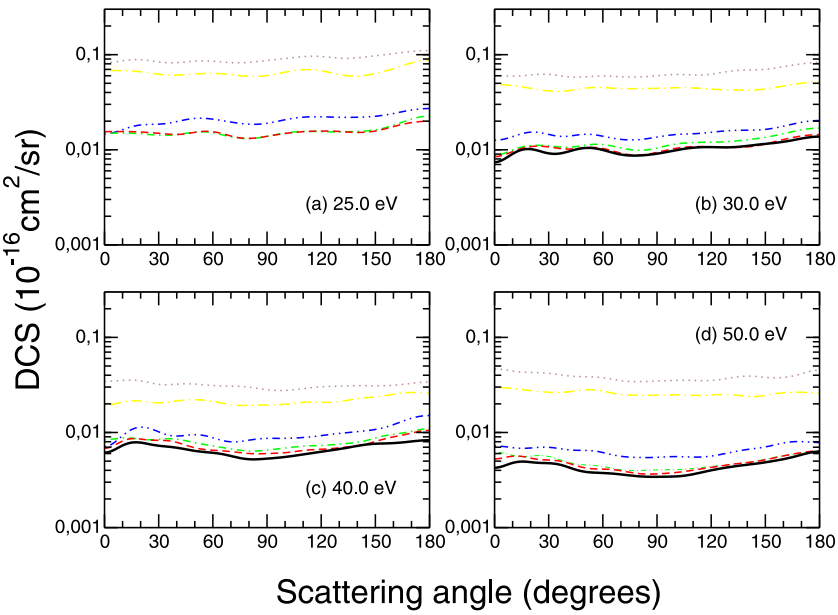

FIG. 13. Influence of the multichannel coupling effects on the electronically inelastic differential cross sections for the third triplet state of furfural for (a) 25.0 eV, (b) 30.0 eV, (c) 40.0 eV, and (d) 50.0 eV electron impact energies with the same legend definitions as in Fig. 6.

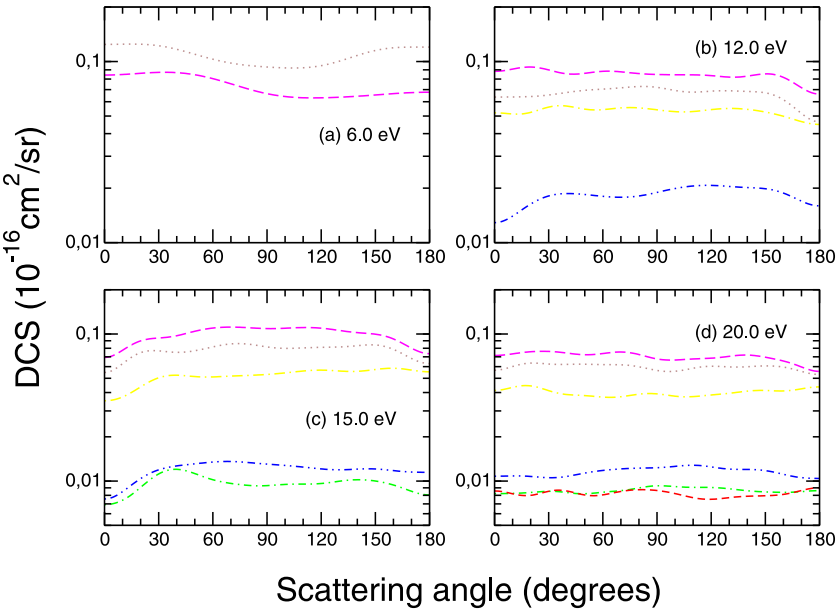

FIG. 14. Influence of the multichannel coupling effects on the electronically inelastic differential cross sections for the first singlet state of furfural for (a) 6.0 eV, (b) 12.0 eV, (c) 15.0 eV, and (d) 20.0 eV electron impact energies with the same legend definitions as in Fig. 5.

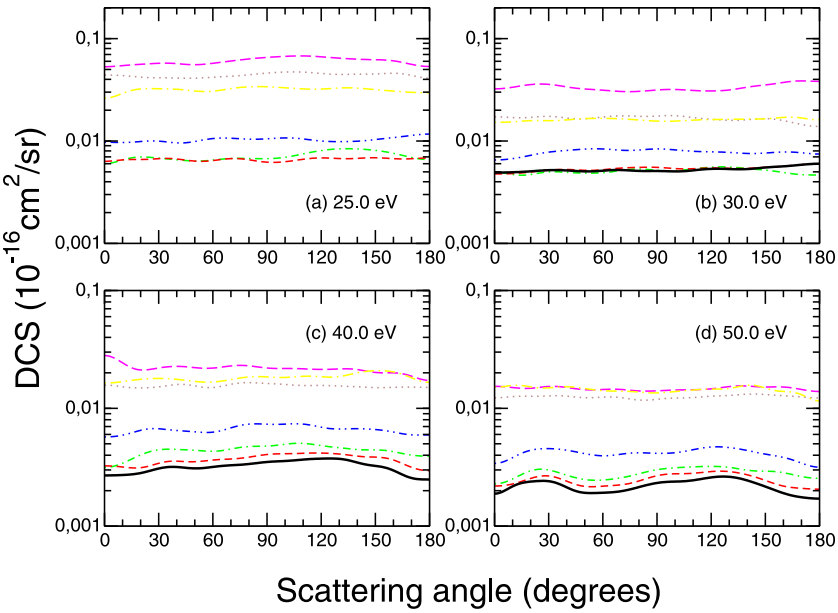

FIG. 15. Influence of the multichannel coupling effects on the electronically inelastic differential cross sections for the first singlet state of furfural for (a) 25.0 eV, (b) 30.0 eV, (c) 40.0 eV, and (d) 50.0 eV electron impact energies with the same legend definitions as in Fig. 6.

state to the first two triplet excited states of furan (namely, the $^3B_2$ and $^3A_1$ excited states)[52,61] indicates that, even with the inclusion of 63-open channels, the electronically inelastic results are not yet fully converged. This point is examined further in Ref. 65.

VI. CONCLUSIONS

We have presented integral-, momentum transfer-, and differential cross sections for elastic and electronically inelastic electron scattering by furfural. Total cross sections were also reported. The results reported in this work represent the most sophisticated application of the SMCPP method in terms of the level of approximation used to incorporate the effects of multichannel coupling. Elastic and total cross section results were also obtained using an improved version of the IAM-SCAR method, which included an interference term that allows for a more realistic description of the collision dynamics. As in our previous applications to ethylene, furan, and phenol, we found that the magnitude of our SMCPP cross sections for furfural are reduced as more channels are included in the scattering calculation. The decrease in magnitude is considerable in going from the 1ch-SEP to the 53ch-SEP level of approximation, while the results obtained at the 53ch-SEP, 57ch-SEP, and 63ch-SE levels of approximation are very similar to each other. In the case of elastic scattering, the results obtained with inclusion of the multichannel coupling effects were in very good agreement with the experimental and other theoretical data for furan and THF available in the literature. Combined together, these findings provide a strong indication that our elastic results could be considered as converged. On the other hand, our SMCPP electronically inelastic cross sections are still bigger than the experimental data for furan, showing that probably even more channels (including discrete electronic as well as ionisation channels) must be included in the scattering calculations.

ACKNOWLEDGMENTS

This work was supported by the Brazilian, Australian, and Spanish governmental funding agencies (CNPq, CAPES, and ARC). R.F.d.C., M.C.A.L., M.H.F.B., M.T.d.N.V., and M.A.P.L. acknowledge support from the Brazilian agency Conselho Nacional de Desenvolvimento Científico e Tecnológico (CNPq). M.T.d.N.V. acknowledges support from Fundação de Amparo à Pesquisa do Estado de São Paulo (FAPESP). D.B.J. thanks the Australian Research Council (ARC) for financial support provided through a Discovery Early Career Researcher Award. M.J.B. thanks the ARC for some financial support and also thanks CNPq for his "Special Visiting Professor" award at the Federal University of Juiz de Fora. G.G. thanks the Spanish Ministerio de Economia y Competitividad under Project No. FIS2012-31230 and the European Union COST Action No. CM1301 for funding. Computational support from CCJDR-IFGW-UNICAMP, where the present SMCPP calculations were performed, is also acknowledged.

[1]*Virtual Biorefinery: An Optimization Strategy for Renewable Carbon Valorization*, edited by A. Bonomi, O. Cavalett, M. P. da Cunha, and M. A. P. Lima (Springer International Publishing, Switzerland, 2016).
[2]J. W. Tester, E. M. Drake, M. J. Driscoll, M. W. Golay, and W. A. Peters, *Sustainable Energy: Choosing Among Options*, 2nd ed. (The MIT Press, Cambridge, MA, 2012).
[3]E. M. de Oliveira, S. d'A. Sanchez, M. H. F. Bettega, A. P. P. Natalense, M. A. P. Lima, M. T. do, and N. Varella, Phys. Rev. A **86**, 020701(R) (2012).
[4]E. M. de Oliveira, R. F. da Costa, S. d'A. Sanchez, A. P. P. Natalense, M. H. F. Bettega, M. A. P. Lima, M. T. do, and N. Varella, Phys. Chem. Chem. Phys. **15**, 1682 (2013).
[5]J. Amorim, C. Oliveira, J. A. Souza-Corrêa, and M. A. Ridenti, Plasma Processes Polym. **10**, 670 (2013).
[6]M. A. Ridenti, J. Amorim, M. J. Brunger, R. F. da Costa, M. T. do N. Varella, M. H. F. Bettega, and M. A. P. Lima, "Electron scattering by biomass molecular fragments: Useful data for plasma applications?," Plasma Sources Sci. Technol. (submitted).
[7]D. B. Jones, G. B. da Silva, R. F. C. Neves, H. V. Duque, L. Chiari, E. M. de Oliveira, M. C. A. Lopes, R. F. da Costa, M. T. do N. Varella, M. H. F. Bettega, M. A. P. Lima, and M. J. Brunger, J. Chem. Phys. **141**, 074314 (2014).
[8]R. F. da Costa, E. M. de Oliveira, M. H. F. Bettega, M. T. do N. Varella, D. B. Jones, M. J. Brunger, F. Blanco, R. Colmenares, P. Limão-Vieira, G. García, and M. A. P. Lima, J. Chem. Phys. **142**, 104304 (2015).
[9]R. F. C. Neves, D. B. Jones, M. C. A. Lopes, K. L. Nixon, G. B. da Silva, H. V. Duque, E. M. de Oliveira, R. F. da Costa, M. T. do N. Varella, M. H. F. Bettega, M. A. P. Lima, K. Ratnavelu, G. García, and M. J. Brunger, J. Chem. Phys. **142**, 104305 (2015).
[10]R. F. C. Neves, D. B. Jones, M. C. A. Lopes, K. L. Nixon, E. M. de Oliveira, R. F. da Costa, M. T. do N. Varella, M. H. F. Bettega, M. A. P. Lima, G. B. da Silva, and M. J. Brunger, J. Chem. Phys. **142**, 194302 (2015).
[11]F. Ferreira da Silva, E. Lange, P. Limão-Vieira, N. C. Jones, S. V. Hoffmann, M.-J. Hubin-Franskin, J. Delwiche, M. J. Brunger, R. F. C. Neves, M. C. A. Lopes, E. M. de Oliveira, R. F. da Costa, M. T. do N. Varella, M. H. F. Bettega, F. Blanco, G. García, M. A. P. Lima, and D. B. Jones, J. Chem. Phys. **143**, 144308 (2015).
[12]D. B. Jones, R. F. C. Neves, M. C. A. Lopes, R. F. da Costa, M. T. do N. Varella, M. H. F. Bettega, M. A. P. Lima, G. García, F. Blanco, and M. J. Brunger, J. Chem. Phys. **143**, 224304 (2015).
[13]R. A. Motiyenko, E. A. Alekseev, S. F. Dyubko, and F. J. Lovas, J. Mol. Spectrosc. **240**, 93 (2006).
[14]B. M. Bode and M. S. Gordon, J. Mol. Graphics Modell. **16**, 133 (1998).
[15]M. A. Khakoo, J. Muse, K. Ralphs, R. F. da Costa, M. H. F. Bettega, and M. A. P. Lima, Phys. Rev. A **81**, 062716 (2010).
[16]K. Takatsuka and V. McKoy, Phys. Rev. A **24**, 2473 (1981); **30**, 1734 (1984).
[17]J. S. dos Santos, R. F. da Costa, and M. T. do N. Varella, J. Chem. Phys. **136**, 084307 (2012).
[18]M. H. F. Bettega, L. G. Ferreira, and M. A. P. Lima, Phys. Rev. A **47**, 1111 (1993).
[19]R. F. da Costa, F. J. da Paixão, and M. A. P. Lima, J. Phys. B **37**, L129 (2004).
[20]R. F. da Costa, M. T. do N. Varella, M. H. F. Bettega, and M. A. P. Lima, Eur. Phys. J. D **69**, 159 (2015).
[21]M. A. P. Lima, T. L. Gibson, K. Takatsuka, and V. McKoy, Phys. Rev. A **30**, 1741 (1984).
[22]Y.-K. Kim and M. E. Rudd, Phys. Rev. A **50**, 3954 (1994).
[23]Y.-K. Kim, W. Hwang, N. M. Weinberger, M. A. Ali, and M. E. Rudd, J. Chem. Phys. **106**, 1026 (1997); M. A. Ali, Y.-K. Kim, W. Hwang, N. M. Weinberger, and M. E. Rudd, *ibid.* **106**, 9602 (1997); H. Nishimura, W. M. Huo, M. A. Ali, and Y.-K. Kim, *ibid.* **110**, 3811 (1999).
[24]H. Tanaka, M. J. Brunger, L. Campbell, H. Kato, M. Hoshino, and A. R. P. Rau, "Scaled plane-wave Born cross sections for atoms and molecules," Rev. Mod. Phys. (in press).
[25]M. C. Fuss, A. G. Sanz, F. Blanco, P. Limão-Vieira, M. J. Brunger, and G. García, Eur. Phys. J. D **68**, 161 (2014).
[26]M. Hoshino, M. Horie, H. Kato, F. Blanco, G. García, P. Limão-Vieira, J. P. Sullivan, M. J. Brunger, and H. Tanaka, J. Chem. Phys. **138**, 214305 (2013).
[27]M. C. Fuss, A. G. Sanz, F. Blanco, J. C. Oller, P. Limão-Vieira, M. J. Brunger, and G. García, Phys. Rev. A **88**, 042702 (2013).
[28]A. G. Sanz, M. C. Fuss, F. Blanco, J. D. Gorfinkiel, D. Almeida, F. Ferreira da Silva, P. Limão-Vieira, M. J. Brunger, and G. García, J. Chem. Phys. **139**, 184310 (2013).
[29]H. Kato, A. Suga, M. Hoshino, F. Blanco, G. García, P. Limão-Vieira, M. J. Brunger, and H. Tanaka, J. Chem. Phys. **136**, 134313 (2012).

[30]H. Kato, K. Anzai, T. Ishihara, M. Hoshino, F. Blanco, G. García, P. Limão-Vieira, M. J. Brunger, S. J. Buckman, and H. Tanaka, J. Phys. B **45**, 095204 (2012).
[31]M. E. Riley and D. G. Truhlar, J. Chem. Phys. **63**, 2182 (1975).
[32]X. Z. Zhang, J. F. Sun, and Y. F. Liu, J. Phys. B **25**, 1893 (1992).
[33]G. Staszewska, D. W. Schwenke, D. Thirumalai, and D. G. Truhlar, Phys. Rev. A **28**, 2740 (1983).
[34]F. Blanco and G. García, Phys. Lett. A **330**, 230 (2004).
[35]F. Blanco and G. García, J. Phys. B **42**, 145203 (2009).
[36]A. Jain, J. Phys. B **21**, 905 (1988).
[37]J. R. Brunton, L. R. Hargreaves, S. J. Buckman, G. García, F. Blanco, O. Zatsarinny, K. Bartschat, and M. J. Brunger, Chem. Phys. Lett. **568-569**, 55 (2013).
[38]J. R. Brunton, L. R. Hargreaves, T. M. Maddern, S. J. Buckman, G. García, F. Blanco, O. Zatsarinny, K. Bartschat, D. B. Jones, G. B. da Silva, and M. J. Brunger, J. Phys. B **46**, 245203 (2013).
[39]P. Palihawadana, J. P. Sullivan, S. J. Buckman, Z. Mašín, J. D. Gorfinkiel, F. Blanco, G. García, and M. J. Brunger, J. Chem. Phys. **139**, 014308 (2013).
[40]F. Blanco and G. García, Chem. Phys. Lett. **635**, 321 (2015).
[41]R. J. Abraham and E. Bretschneider, in *Internal Rotation in Molecules*, edited by W. J. Orville-Thomas (Wiley, New York, 1974), pp. 481–584.
[42]M. W. Schmidt, K. K. Baldridge, J. A. Boatz, S. T. Elbert, M. S. Gordon, J. H. Jensen, S. Koseki, N. Matsunaga, K. A. Nguyen, S. J. Su, T. L. Windus, M. Dupuis, and J. A. Montgomery, J. Comput. Chem. **14**, 1347 (1993).
[43]*CRC Handbook of Chemistry and Physics*, 79th ed., edited by D. R. Lide (CRC, Boca Raton, USA, 1998).
[44]D. B. Jones, E. Ali, K. L. Nixon, P. Limão-Vieira, M.-J. Hubin-Franskin, J. Delwiche, C. G. Ning, J. Colgan, A. J. Murray, D. H. Madison, and M. J. Brunger, J. Chem. Phys. **143**, 184310 (2015).
[45]J. de Urquijo, E. Basurto, A. M. Juárez, K. F. Ness, R. E. Robson, M. J. Brunger, and R. D. White, J. Chem. Phys. **141**, 014308 (2014).
[46]C. Winstead and V. McKoy, Phys. Rev. A **57**, 3589 (1998).
[47]C. W. Bauschlicher, Jr., J. Chem. Phys. **72**, 880 (1980).
[48]F. Kossoski, M. H. F. Bettega, and M. T. do N. Varella, J. Chem. Phys. **140**, 024317 (2014).
[49]S. W. Staley and J. T. Strnad, J. Phys. Chem. **98**, 116 (1994).
[50]C. Winstead and V. McKoy, Phys. Rev. Lett. **98**, 113201 (2007).
[51]A. S. Barbosa, D. F. Pastega, and M. H. F. Bettega, Phys. Rev. A **88**, 022705 (2013).
[52]R. F. da Costa, M. H. F. Bettega, M. A. P. Lima, M. C. A. Lopes, L. R. Hargreaves, G. Serna, and M. A. Khakoo, Phys. Rev. A **85**, 062706 (2012).
[53]C. J. Colyer, V. Vizcaino, J. P. Sullivan, M. J. Brunger, and S. J. Buckman, New J. Phys. **9**, 41 (2007).
[54]M. Dampc, A. R. Milosavljević, I. Linert, B. P. Marinković, and M. Zubek, Phys. Rev. A **75**, 042710 (2007).
[55]M. Allan, J. Phys. B: At., Mol. Opt. Phys. **40**, 3531 (2007).
[56]A. Gauf, L. R. Hargreaves, A. Jo, J. Tanner, and M. A. Khakoo, Phys. Rev. A **85**, 052717 (2012).
[57]C. S. Trevisan, A. E. Orel, and T. N. Rescigno, J. Phys. B: At., Mol. Opt. Phys. **39**, L255 (2006).
[58]C. Winstead and V. McKoy, J. Chem. Phys. **125**, 074302 (2006).
[59]C. Szmytkowski, P. Mozejko, E. Ptasińska-Denga, and A. Sabisz, Phys. Rev. A **82**, 032701 (2010).
[60]A. Zecca, C. Perazzolli, and M. J. Brunger, J. Phys. B: At., Mol. Opt. Phys. **38**, 2079 (2005).
[61]K. Regeta and M. Allan, Phys. Rev. A **91**, 012707 (2015).
[62]A. R. Milosavljević, A. Giuliani, D. Šević, M.-J. Hubin-Franskin, and B. P. Marinković, Eur. Phys. J. D **35**, 411 (2005).
[63]W. Y. Baek, M. Bug, H. Rabus, E. Gargioni, and B. Grosswendt, Phys. Rev. A **86**, 032702 (2012).
[64]J. B. Maljković, F. Blanco, R. Curik, G. García, B. P. Marinković, and A. R. Milosavljević, J. Chem. Phys. **137**, 064312 (2012).
[65]D. B. Jones, R. F. C. Neves, M. C. A. Lopes, R. F. da Costa, M. T. do N. Varella, M. H. F. Bettega, M. A. P. Lima, G. García, P. Limão-Vieira, and M. J. Brunger, J. Chem. Phys. **144**, 124309 (2016).